



Nano-curcumin versus curcumin in amelioration of deltamethrin-induced hippocampal damage

Sherif Mohamed Zaki^{1,2} · Waleed Ahmed Abd Algaleel^{1,6} · Reda Abdelnasser Imam^{1,6} · Ghada F. Soliman^{3,6} · Fatma M. Ghoneim^{4,5}

Accepted: 10 March 2020 / Published online: 29 March 2020
© Springer-Verlag GmbH Germany, part of Springer Nature 2020

Abstract

We aimed to prove that oxidative stress is the main mechanism responsible for hippocampal neurotoxicity induced by deltamethrin (DLM). The protective role of curcumin (CMN) and nano-curcumin (NCMN) over this toxicity was studied. The rats were categorized into four groups: control, DLM, CMN and NCMN. The study continued for 30 days. Hippocampus was processed for histological, biochemical and immunohistochemical studies. Caspase-3, glial fibrillar acidic protein (GFAP), acetylcholinesterase (AChE), malondialdehyde (MDA), glutathione (GSH), catalase (CAT) and superoxide dismutase (SOD) were measured for DLM-induced oxidative stress (increased MDA by 354%/decreased GSH by 61%, SOD by 61%, CAT 57%). Oxidative stress induced apoptosis of hippocampal neurons through increasing Nrf2, gamma-glutamyl cysteine synthetase heavy subunit (GCS-HS) and light subunit (GCS-LS) and decreasing AChE. It increases the activity of astrocytes through increasing GFAP. Finally, oxidative stress has a bad impact on cognitive function. Improvement of oxidative stress was observed with use of CMN and NCMN (decrease of MDA/increase of GSH, SOD, CAT). The level of Nrf2, GCS-HS and GCS-LS decreased, while AChE, GFAP increased. Improvement of cognitive function was observed in both groups. In conclusion, oxidative stress is the common mechanism responsible for DLM-induced hippocampal neurotoxicity. It exerts apoptosis of hippocampal neurons through increasing Nrf2, HS-GCS, LS-GCS and decreasing AChE. In addition, it activates astrocytes through increasing expression of GFAP. The protective role of CMN and NCMN is related to their potent antioxidant effect. Much improvement has been detected with NCMN as compared to CMN.

Keywords Nano-curcumin · Curcumin · Deltamethrin · Hippocampus

Introduction

Deltamethrin (DLM) is a type II pyrethroid (Breckenridge et al. 2009). Pyrethroids are the most commonly used pesticides and are extensively used insecticides in indoor environments (Saillenfait et al. 2015). They are found in many agriculture's preparations, pet shampoos and scabies-treating medication (Saillenfait et al. 2015). Their usage has increased in the last 2 decades due to their efficacy and restrictions on the use of organophosphates (Williams et al. 2008).

Pyrethroids are lipophilic compounds that cross the blood–brain barrier and reach the brain at neurotoxic concentrations (Wozniak et al. 1990). The relation between long-term exposure to pyrethroids and neurobehavioral disorders was recognized in many works (Wagner-Schuman et al. 2015; Richardson et al. 2015). Type I compounds induce T (tremor) syndrome, while type II

✉ Sherif Mohamed Zaki
zakyshef1@gmail.com

¹ Department of Anatomy and Embryology, Faculty of Medicine, Cairo University, Giza, Egypt

² Present Address: Fakeeh College for Medical Sciences, Jeddah, Saudi Arabia

³ Department of Pharmacology, Faculty of Medicine, Cairo University, Giza, Egypt

⁴ Department of Histology and Cell Biology, Faculty of Medicine, Mansoura University, Mansoura, Egypt

⁵ Present Address: Faculty of Medicine, Mansoura University, Mansoura, Egypt

⁶ Present Address: Faculty of Medicine, Cairo University, Giza, Egypt

compounds cause CS (choreoathetosis and salivation) syndrome (Verschoyle and Aldridge 1980; Ray 1982). Unlike other pyrethroids, DLM has no peripheral nervous effect (Wolansky and Harrill 2008), as CNS represents its main neurotoxic goal (Wolansky and Harrill 2008). In vitro studies have revealed that DLM affects differentially neuronal subtypes in hippocampus (Grosse et al. 2002) and induces apoptotic cell death in cultured cerebro-cortical neurons (Wu et al. 2003). In vivo studies have shown that DLM modifies the expression of P 53, Bax Bcl-2 in rat brain (Wu et al. 2000) and inhibits the dopaminergic and cholinergic neurotransmission mechanisms (Wu et al. 2000; Hossain et al. 2005). The mechanisms of the toxicity of pyrethroids are linked to induction of oxidative stress, production of free radicals, increased lipid peroxidation, and disruption of the total antioxidant potential (Radovanović et al. 2017).

Hippocampus is a major component of the brain. It is involved in memory forming, organizing, and storing (Arisi 2014). Hippocampus is a target organ of DLM neurotoxicity (Huang et al. 2019). Inducing apoptosis of hippocampal neurons is one of mechanisms by which DLM induces neurotoxicity which finally leads to impairment of learning and memory (Gasmi et al. 2017; Nieradko-Iwanicka and Borzęcki 2015).

Curcumin (CMN) is derived from the rhizomes of *Curcuma longa* turmeric and is used as a spice and food coloring agent (Menon and Sudheer 2007). It has antioxidant, anti-inflammatory and immunomodulatory properties (Menon and Sudheer 2007). It exhibits its antioxidant effect through free radical-scavenging activity (Kocaadam and Şanlier 2017). CMN has a protective role against oxidative stress-mediated neuropathy, cardiomyopathy, nephropathy, retinal neurodegeneration, testicular dysfunction and hepatic injury (Yan et al. 2017; Rashid and Sil 2015; Mandal et al. 2009). There are many challenges that limit the clinical application of CMN, among which are its poor aqueous solubility, poor bioavailability in organs photodegradation, chemical instability, rapid metabolism, and short half-life (Lu et al. 2015; Huang et al. 2015; Anand et al. 2007). Nano-curcumin (NCMN) provides a very efficient solution. Nano-emulsions are nano-carriers that represent a very promising delivery system for CMN (Onoue et al. 2010). Its oral absorption efficacy is 40-fold greater than that of CMN in both rats and humans (Sasaki et al. 2011) and has a better pharmacokinetic profile (Onoue et al. 2010).

We hypothesized that DLM induces adverse hippocampal damage through oxidative stress. So, we aimed to prove that oxidative stress is the common mechanism responsible for hippocampal neurotoxicity induced by DLM. We also compared the protective role of CMN and NCMN over this toxicity. Morris water maze was used to determine the hippocampal-dependent learning affection.

Materials and methods

Animals

Wistar albino rats were obtained from the Animal House, Faculty of Medicine, Cairo University. The rats were housed in 12 h dark–light manner with food and water available ad libitum.

The experimental design was in accordance with the guidelines of the Institutional Animal Care and Use Committee (CU-IACUC), Cairo University (CU-III-F-40-19). The work complied with the ARRIVE guidelines and was carried out in accordance with the U.K. Animals (Scientific Procedures) Act 1986 and associated guidelines, EU Directive 2010/63/EU for animal experiments. The study was done according to the ethical standards of the National Institutes of Health guide for the care and use of Laboratory Animals (8th edition, revised in 2011).

Test materials

Deltamethrin was obtained from Chem Service Inc, West Chester, PA. DLM was dissolved in the corn oil and administered via oral gavage at $1/10$ of LD_{50} (15 mg/kg) once daily for 30 days (Sharma et al. 2014). The LD_{50} value for DLM is 128 mg/kg (based on administration of the compound in the corn oil) (Frank et al. 2000). The repeated exposure for 1 month was chosen to represent subacute exposure (Klaassen et al. 2010).

Curcumin was purchased from Sigma-Aldrich (St. Louis, MO, USA). The dose of CMN (2.5 mg/kg BW) was selected from the study of Kalpana and Menon (Kalpana and Menon 2004). CMN was dissolved in dextrose 5% and administered via gavage.

Nano-curcumin was purchased from Nanotech Egypt for photoelectronic communication Center. The dose of NCMN was 2.5 mg/kg BW (the same dose of CMN to compare the potency of both components). NCMN was dissolved in dextrose 5% and administered via gavage.

NCMN was prepared by slightly modifying the method of Basniwal (Bhawana et al. 2011). For synthesis of NCMN, a solution was prepared by dissolving 0.018 M curcumin in 30 mL dichloromethane. It was mixed dropwise (flow rate 0.2 mL/min) in warm (50 °C) Milli-Q ultrapure water for 10 min under ultrasonic-pulse sonication conditions with a constant stirring at 600 rpm (Hielscher Ultrasonic Processor- UP100H, Germany). The colored solution containing NCMN was separated by centrifugation. It was autoclaved and then freeze-dried at 2808 °C. After that, the sample was lyophilized (EYELA-FDU-2000, Japan) to obtain a dry orange powder of NCMN.

Health status and general toxicological profile

General toxicological data were recorded including food and water consumption, motility, and health status. The body weight was recorded at beginning and end of work.

Morris water maze (MWM) (Nunez 2008; Hossain et al. 2005)

MWM was used to evaluate the rats' ability to store and manage spatial information [escaping the aversive situation (pool water) and reaching the refuge as quickly as possible]. Data were acquired and analyzed with a live video tracking system.

The maze consisted of a circular pool (100 cm diameter \times 30 cm height) filled with water at 23 ± 1 °C (the relatively low-temperature water gives the test aversive nature). Water was made white opaque with powdered milk (Cat # 902887, MP Biomedicals, Solon, OH). The hidden platform (5 cm diameter \times 18 cm height) was submerged 1.5 cm below the water surface. The maze was positioned in a room with external landmarks which are large colored papers fixed to the wall and visible to the swimming animal. The external landmarks are arranged as the following; N.: white square, S.: green diamond, E.: yellow triangle and W.: blue circle. These landmarks were to create a geographical map and to navigate the platform site. The platform was placed in the middle of the east quadrant and remained in the same position during acquisition.

During acquisition, each animal had four trials daily at 1-min interval for 7 days. Each animal was released from one of the quadrants facing the wall of the pool. The order of the start location was rotated every trial as south–west–north–south and each trial lasted until the animal found the platform within 60 s and remained on the platform for 30 s. If the animal failed to find the platform within 60 s, it was placed on the platform for 30 s. At the end of each trial, rats were removed, dried and placed in cages under heating lamps until the next trial.

A visual cue test was performed at beginning of training (day 1) and end of the last session (day 7) to identify whether there were any visual or motor deficits that impaired the rats' performance. For this test, the platform was set one above the water level and marked with black tape so that the rats could locate the platform via a local visual stimulus rather than depending on spatial orientation to extra-maze cues.

Experimental design

Thirty-two Wistar rats were randomly categorized into four groups: control group, DLM-treated group, CMN-treated group (DLM and CMN were given concomitantly) and NCMN-treated group (DLM and NCMN were given

concomitantly). The sample size was based according to the resource equation method. The study continued for 30 days (subacute intoxication). Then, all rats were sacrificed. Hippocampus was processed for biochemical, histological, and immunohistochemical study.

Tissue sampling

The hippocampus was dissected and fixed immediately in 10% formalin saline. Hippocampal subfields (CA1, CA2, CA3) were manually outlined on each slice using the Aperio Image Scope[®] CS (Suvarna et al. 2019). To randomize selection, every tenth section (5 μ m thick) was put aside for staining.

Light microscopic study

The hippocampal sections were stained with hematoxylin and eosin (H&E) and cresyl violet stains. The stained sections were examined using Leica microscope and photographed using a Canon digital camera connected to an IBM computer system. Image analysis was performed using the software Leica Quin 500, Germany.

Cresyl violet staining (Nissl staining) (Zhu et al. 2015; Suvarna et al. 2019)

This method is used for the recognition of Nissl body in the cytoplasm of neurons, to recognize the basic neuronal structure from necrotic neurons in hippocampus. The slide-mounted hippocampal sections were differentiated in 95% ethyl alcohol for 5 h before staining, rinsed in 75% ethyl alcohol for 5 min and in distilled water for 5 min. Next, the sections were stained in 0.1% cresyl violet (Sigma) solution for 2–3 min and then rinsed quickly in distilled water. After decolorization in 75% ethyl alcohol, the sections were dehydrated in 95%, 100% ethyl alcohol for 2 min, cleared in xylene for 2–3 min and mounted with Permount (Fisher Scientific) in a fume hood. The amount of the cell in the hippocampus area (mm^2) was calculated by Optilab Image Raster software.

Immunohistochemical study (Suvarna et al. 2019)

Deparaffinized sections were processed for immunohistochemistry for caspase-3 and glial fibrillar acidic protein (GFAP) markers. Avidin–biotin immunohistochemical staining technique was done according to the manufacturer's instructions. The kit was supplied by Dako (catalog no. M0724) and the clone was DE-R-11. The primary antibodies against DLM were GFAP at a 1:2500 dilution (ab7260) and caspase-3 at a 1:1000 dilution (ab13847).

The second, fourth, sixth, eighth, tenth, twelfth and fourteenth consecutive coronal sections containing hippocampus were put on positively charged glass slides. Paraffin sections were deparaffinized, hydrated, and then put in 10% H_2O_2 to block endogenous peroxidase activity. Unmasking of antigenic sites was carried out by transferring the sections into a jar containing 0.001 M citrate buffer (pH 6) and then boiling in a microwave for 4 min at temperature grade VIII, followed by 2 min at grade II. Incubation with 1/100 normal rabbit serum for 20 min was carried out to block the nonspecific background staining. The diluted goat anti-rat primary antibody was then added on the slides and kept for 2 h. The slides were then washed with PBS and 1/400 biotinylated rabbit anti-goat IgG secondary antibody was then added to the slides and kept for 1 h. Streptavidin peroxidase was then added to bind with biotin residue on the linking antibody for 10 min and then washed with PBS. The site of antibody immunostaining was visualized using the avidin–biotin–peroxidase complex (ABC reagent) for 30 min. Freshly prepared diaminobenzidine was used as chromogen. The sections were incubated with diaminobenzidine for 10 min and then washed with tap water, dehydrated, and mounted. Positive control for GFAP and caspase-3 was IHC-Fr: rat brain tissue.

Quantitative morphometric study for caspase-3 and astrocyte-positive cell

The dark brown caspase-3-positive cells and dark brown immunoreactive astrocytes from different hippocampal regions were visualized using a Leica Qwin 500 image analyzer computer system (England). The positive cells were counted at higher magnification from a total of six sections per animal and three animals/group (Hossain et al. 2015). The number of caspase-3- and GFAP-positive cells was measured manually using digital photomicrographs.

Biochemical analysis

Hippocampal homogenates were processed for estimation of MDA, GSH, CAT, SOD and acetylcholinesterase (AChE) activity by ELISA kits supplied by My BioSource, USA.

Malondialdehyde (MDA), an oxidative stress and a lipid peroxidation marker, was measured according to Tipple and Rogers (Tipple and Rogers 2012). 100 mg of hippocampal tissue was homogenized in 1 mL of PBS, pH 7.0 with a micropestle in a microtube. 20% trichloric acid solution was added to the tissue homogenate to precipitate the protein and centrifuged. 0.8% thiobarbituric acid solution was added to the supernatants. After boiling for 10 min, the absorbance was measured at 405 nm. The concentration of MDA was calculated using the standard curve and expressed per mg of protein (U/mg protein).

Tissue glutathione (GSH) content was measured according to Tipple and Rogers (Tipple and Rogers 2012). The measurement was based on the reduction of diaminobenzidine (DAB) with reduced glutathione to produce a yellow compound. DAB-stained pixels were selected by setting a threshold on the blue channel values. The reduced chromogen was directly proportional to GSH concentration and its absorbance was measured at 405 nm. Concentration of GSH was expressed per mg of protein (U/mg protein).

Catalase (CAT) activity was measured according to Aebi's method (Aebi 1984). Twenty microliters of 10% hippocampal homogenate was added to a cuvette containing 780 μ L of sodium phosphate buffer and 200 μ L of hydrogen peroxide (H_2O_2 , 3%). Catalase activity was measured at 240 nm for 3 min using a spectrophotometer. The activity of one unit is equal to the μ moles of H_2O_2 degraded per minute per milligram of protein (μ mol/ H_2O_2 utilized/min/mg protein).

Superoxide dismutase (SOD) activity was evaluated according to the modified Misra and Fridovich's method (Misra and Fridovich 1972). Five microliters of 10% hippocampal homogenate was added to 1965 μ L of sodium carbonate buffer and to ten microliters of bovine catalase. Twenty microliters of 30 mM epinephrine were added to the mixture. SOD activity was measured at 480 nm for 5 min on a spectrophotometer. The activity was expressed as the amount of the enzyme that inhibits the oxidation of epinephrine by 50%, which is equal to 1 U per milligram of protein.

AChE activity was measured according to the Ellman method (ELLMAN et al. 1961). 3 mL of 5,50-dithiobis-2-nitrobenzoic acid (DTNB) prepared in 0.01% buffered isotonic saline solution and 0.9 mL of acetylthiocholine iodide solution were added to 0.3 mL 10% hippocampal homogenate. This mixture was incubated at 37 °C for 20 min. 0.3 mL of eserine salicylate solution was added and mixed to stop the enzymatic reaction. The absorbance was determined at 405 nm. AChE activities were calculated from standard curve prepared using different concentrations of reduced glutathione at 412 nm. AChE activity is stated as μ mol product per mg of protein (U/mg protein).

Gene expression of gamma-glutamyl cysteine synthetase heavy (GCS-HS) and light (GCS-LS) subunits, NF-E2-related factor 2 (Nrf2) using RT-PCR

Total RNA extraction

Total RNA was extracted from hippocampal tissues using the TRIzol method according to the manufacturer's protocol. RNA was removed by homogenization in TRIzol reagent (Invitrogen, Life Technologies, USA). The tissue homogenate was then incubated for 5 min. A 1:5 volume of chloroform was added and the tube was vortexed and centrifuged at

12 000 g for 15 min. The aqueous phase was isolated and the total RNA was precipitated with absolute ethanol. The total RNA was finally eluted in 20 μ L of the RNase-free water. The RNA concentrations and purity were measured with an ultraviolet spectrophotometer.

Complementary DNA (cDNA) synthesis

The cDNA was synthesized from one μ g RNA using SuperScript III First-Strand Synthesis System as described in the manufacturer's protocol (Invitrogen, Life Technologies). In brief, 1 μ g of total RNA was mixed with 50 μ M oligo (DT) 20, 50 ng/ μ L random primers, and 10 mM dNTP mix in a total volume of 10 μ L. The mixture was incubated at 56 °C for 5 min and then placed on ice for 3 min. The reverse transcriptase master mix containing 2 μ L of 10 \times RT buffer, 4 μ L of 25 mM MgCl₂, 2 μ L of 0.1 M DTT, and 1 μ L of SuperScript[®] III RT (200 U/ μ L) was added to the mixture and was incubated at 25 °C for 10 min followed by 50 min at 50 °C.

Real-time quantitative PCR

The relative abundance of mRNA species was assessed using the SYBR Green method on an ABI prism 7500 sequence detector system (Applied Biosystems, Foster City, CA). PCR primers were designed with Gene Runner Software (Hasting Software, Inc., Hasting, NY) from RNA sequences from Gen Bank. All primer sets had a calculated annealing temperature of 60°. Quantitative RT-PCR was performed in a 25- μ l reaction volume consisting of 2X SYBR Green PCR

Master Mix (Applied Biosystems), 900 nM of each primer and 2–3 μ l of cDNA. The PCR amplification consisted of an initial denaturation for 5 min at 95 °C, followed by 35 cycles of 30 s denaturation at 95 °C, annealing for 30 s at 50 °C and extension for 2 min at 72 °C. The final extension step was carried out at 72 °C for 7 min. Data from real-time assays were calculated using the v1.7 Sequence Detection Software from PE Biosystems (Foster City, CA). Relative expression of studied gene mRNA was calculated using the comparative Ct method. All values were normalized to the beta actin gene and reported as fold change over background levels detected in diseases group.

Western blotting analysis (Li et al. 2013)

Protein samples were resolved on 10% SDS polyacrylamide gels and were transported to nitrocellulose membranes. Membranes were blocked in Tris-buffered saline (TBS) with 0.1% Tween-20 and 5% nonfat dry milk for 1 h. After that, they were incubated overnight with primary antibodies diluted in the identical buffer. Nrf2 was used in the dilution of 1:500 and GAPDH in the dilution of 1:8000. After the washing with 0.1% Tween-20 in TBS, the membranes were incubated with peroxidase-conjugated secondary antibodies for 1 h and then rinsed and developed using the ECL chemiluminescent detection system. Blots were then visualized with X-ray films. The results were analyzed using the Band Scan 4.3 software. Densitometry was normalized against the signal obtained from coinubation with anti-GAPDH.

Primer sequence used in the study

Table 1 Comparison of the body weight among the different groups at the end of study

Group	BW (g) Mean \pm SD	Minimum	Maximum	Versus group	<i>P</i> value
Control	270.3 \pm 15.8	250	290	DLM-treated	0.000*
				CMN-treated	0.001*
				NCMN-treated	1.000
DLM-treated	220 \pm 7.9	210	230	Control	0.000
				CMN-treated	0.05*
				NCMN-treated	0.000*
CMN-treated	238.6 \pm 6.1	230	245	Control	0.001*
				DLM-treated	0.05*
				NCMN-treated	0.009*
NCMN-treated	262.2 \pm 5.6	255	270	Control	1.000
				DLM-treated	0.000*
				CMN-treated	0.009*

The mean weight \pm SD at the beginning of the study was 215 \pm 11 g, minimum 190 g, 235 g

*Significant

Gene	Primer sequence
GCS-LS	Forward primer: 5'-GCACAAAGC GCTGAGTCA CGGG-3' Reverse primer: 5'-GCCCGTGAC TCAGCGCTT TGTG-3'
Nrf2	Forward primer: 5'-CCATTTACG GAGACCCAC-3' Reverse primer: 3'-CTTATTCA ACGGCGAGT-5'

Statistical analysis

Statistical analysis was performed using statistical package for the social sciences (SPSS) version 21.0 (IBM Corporation, Somers, NY, USA) statistical software. The data were expressed as mean \pm standard deviation (SD). Statistical evaluation was done using one-way analysis of variance (ANOVA) followed by Bonferroni pairwise comparisons. Significance was considered when the *p* value was less than 0.05.

The percentage of increase or decrease (difference) of all study parameters was calculated per the following formula: Percentage of difference = (Mean difference value between two groups)/(Value of the compared group) \times 100.

Results

General toxicological profile and mortality (Table 1)

The DLM-treated rats looked sicker compared to other treated animals. Five rats died during the study: three from the DLM-treated group, one from the CMN-treated group and one from the NCMN-treated group.

At the beginning of the study, the rats' weight was 215 ± 11 g. At the end of experiment, weight of the DLM-treated group was 18.5% lower than that of the control group. Weight of the CMN- and NCMN-treated groups was 8.1 and 19% higher than that of the DLM-treated group. Compared to that of the CMN-treated group, weight of the NCMN-treated group was 10% higher.

Structure of hippocampus as revealed by H&E staining (Figs. 1–3)

The control group presented normal hippocampal morphology. The hippocampal areas are CA1, 2 and 3. The

Fig. 1–3 **a** Normal pyramidal neurons of the control rats. **b** Degenerated and vacuolated pyramidal neurons (arrowhead), apoptotic pyramidal neurons (arrows) in the DLM-treated rats. **c** Normal pyramidal neurons (P), degenerated and vacuolated pyramidal neurons (arrowheads), apoptotic pyramidal neurons (arrows) in the CMN-treated rats. **d** Normal pyramidal neurons (P) of the NCMN-treated rats. H & E, scale bar, 50 μ m (**a–d**)

hippocampal layers are polymorphic, pyramidal and molecular. Pyramidal neurons had larger cell bodies and only one nucleolus.

CA1, 2, 3 areas of DLM-treated rats exhibited degenerated, vacuolated and apoptotic pyramidal neurons. This was a consistent result in all specimens that suggests a highly impaired general organ condition after the treatment with DLM. Improvement of pyramidal neurons was observed in CMN- and NCMN-treated groups. Few apoptotic pyramidal neurons were seen in the CMN-treated group, while the neurons in the NCMN-treated group were nearly normal.

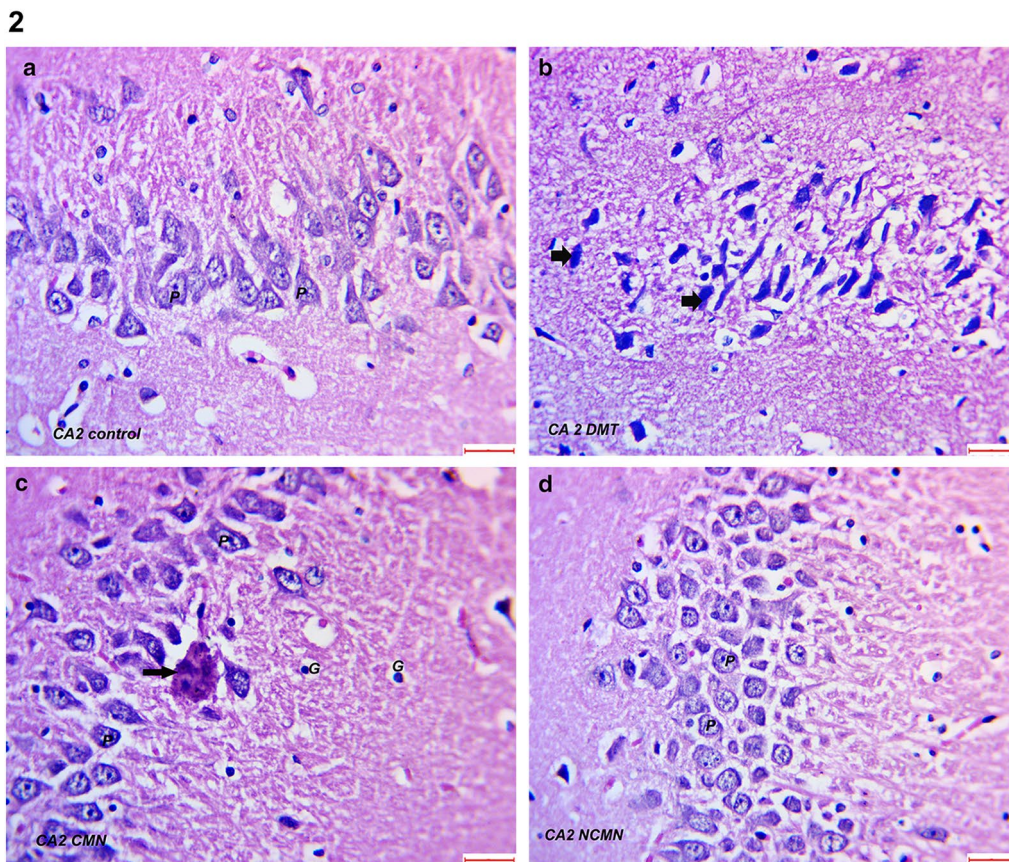
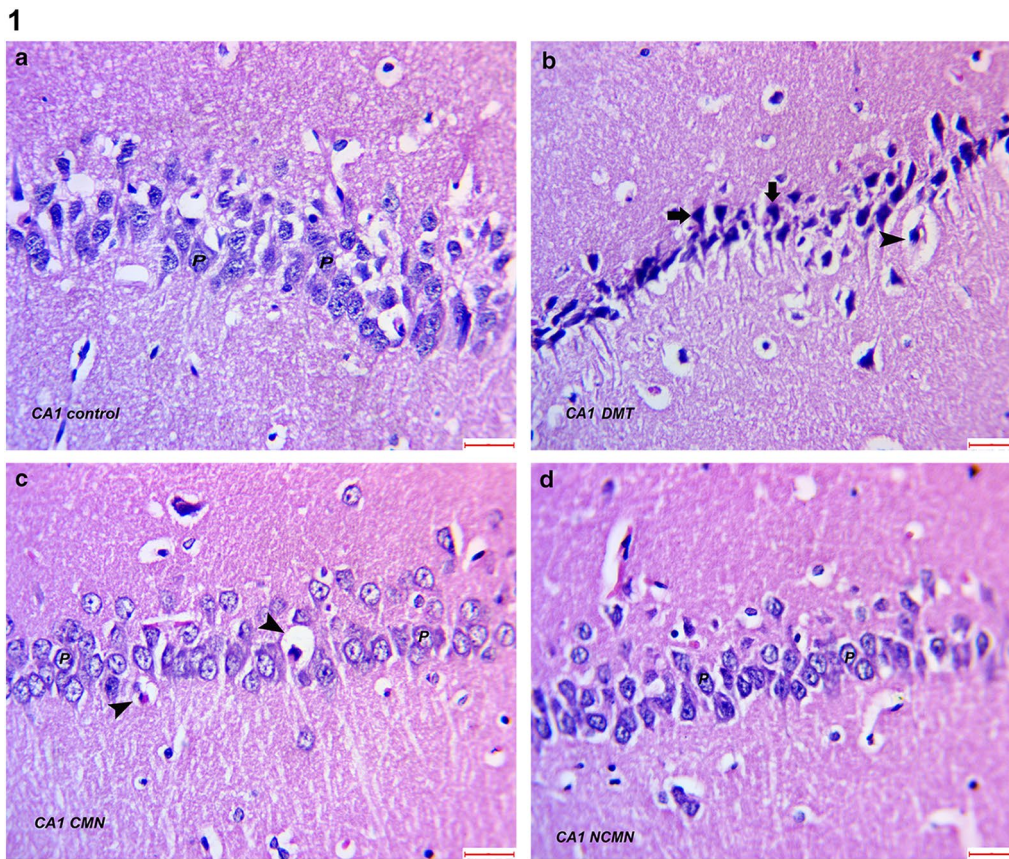
Structure of hippocampus as revealed by cresyl violet staining

Pyramidal neurons showed their normal appearance in the control group with normal Nissl bodies staining. With use of DLM, pyramidal neurons exhibited degeneration and shrinkage with strong Nissl bodies staining. Little degeneration of pyramidal neurons with normal Nissl bodies staining was realized in CMN-treated group. Pyramidal neurons of NCMN-treated group were nearly completely normal (Fig. 4).

Pyramidal cell density in the CA1 and CA3 area decreased significantly as compared to other groups. A significant improvement in the pyramidal cell density was observed in CMN- and NCMN-treated groups as compared to that of the other two groups. The improvement in NCMN-treated group was better than that of CMN-treated group (Fig. 5).

Caspase-3 immunohistochemistry

Caspase-3 immunohistochemistry proved the presence of dark brown immunoreactive apoptotic pyramidal neurons (Fig. 6). DLM increased apoptotic pyramidal neurons (eightfold increase) as compared to that of control group. Improvement was observed with use of CMN, as there was a threefold increase in the number of apoptotic neurons as compared to that of control group. A non-significant difference was observed between NCMN-treated group and control group (Table 2).



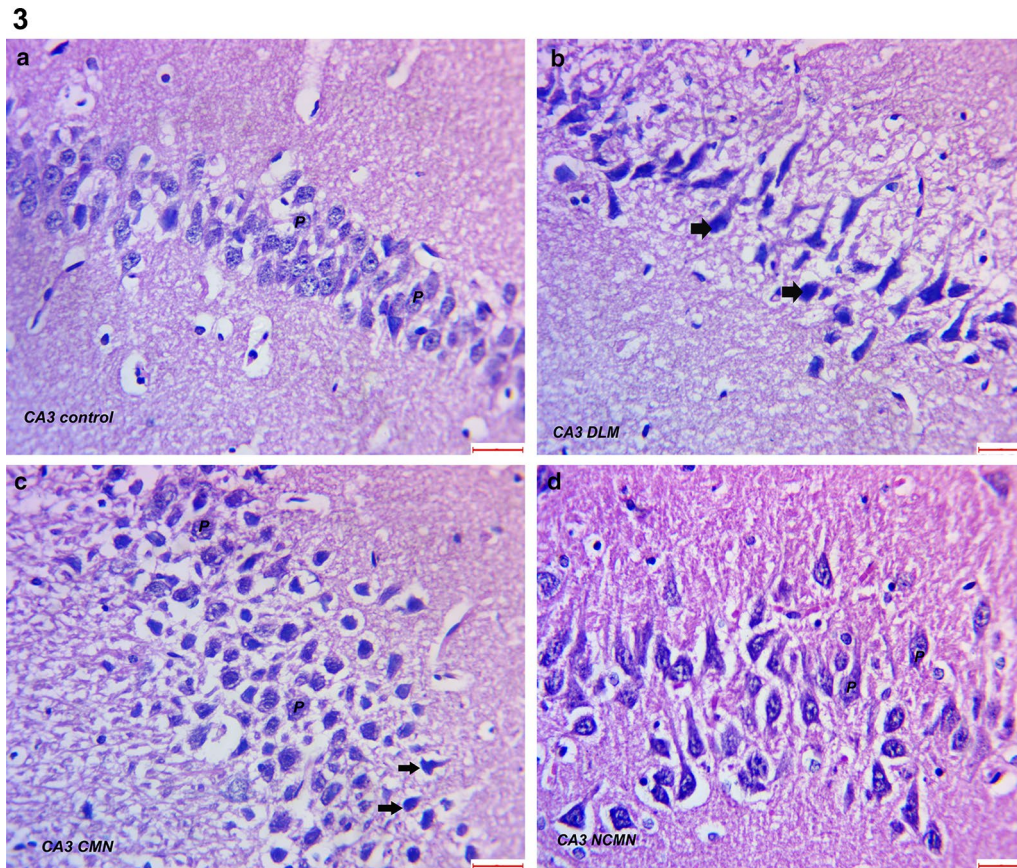


Fig. 1–3 (continued)

GFAP immunohistochemistry

GFAP immunohistochemistry exhibited the presence of dark brown immunoreactive astrocytes in different hippocampal regions (Fig. 7). Treatment with DLM significantly increased the number of GFAP-immunoreactive astrocytes (176%) as compared to that of control group. Much improvement was observed with use of CMN (85% increase in the number of GFAP) as compared to that of control group. A non-significant difference was observed between NCMN-treated group and control group (Table 2).

Level of oxidant/antioxidant markers (Table 3)

DLM promoted lipid peroxidation. The level of MDA in hippocampal homogenates increased in DLM-treated group by 354% as compared to that of the control group. With use of CMN and NCMN, MDA decreased by 38, 60% as compared to that of DLM-treated group. However, MDA in both groups was still higher than that of control group (178, 80%, respectively).

Administration of DML decreased the level of antioxidant markers. Compared to the control rats, DML-treated animals

showed a decrease in GSH, SOD and CAT by 61, 61, and 57%, respectively. With use of CMN and NCMN, levels of GSH increased by 69, 125%, SOD increased by 61, 135% and CAT increased by 80, 118% compared to their similarities of DLM-treated group. The increased level was more prominent in NCMN-treated group. The level of all markers of NCMN-treated group reached their similarities of the control group.

Level of AChE, GCS-LS, GCS-HS and Nrf2 (Table 4, Fig. 8)

Administration of DLM reduced the level of AChE by 50% compared to that of the control group. With use of CMN and NCMN, the enzyme level increased by 50, 75% compared to that of DLM-treated group. However, the enzyme level in the last two groups did not reach the level of control group (25 and 13% lower, respectively).

With use of DLM, the mRNA expression of GCS-LS and GCS-HS increased by 140, 104% compared to that of the control group. With use of CMN and NCMN, the level of GSH-LS decreased by 46 and 44% and the level of GCS-HS decreased by 20% compared to that of DLM-treated group.

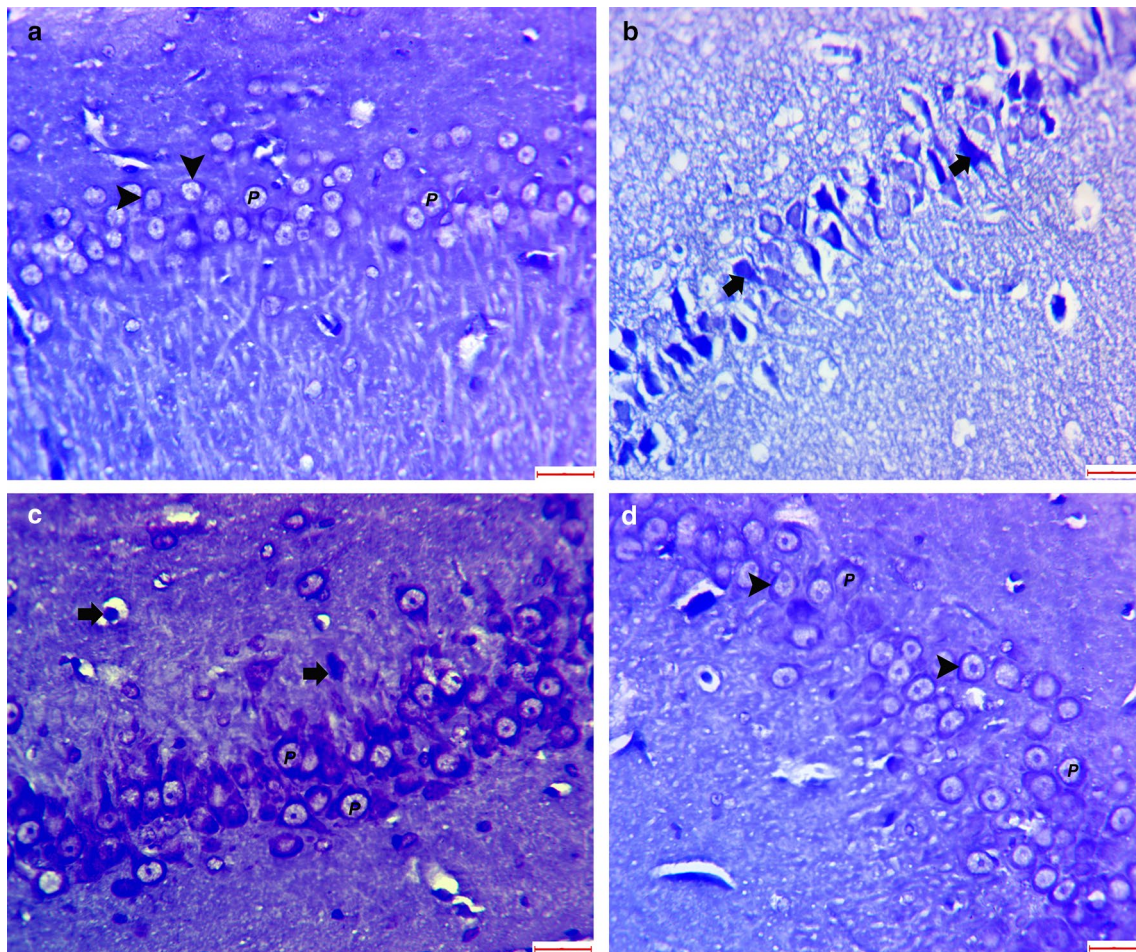


Fig. 4 **a:** Normal pyramidal neurons (P) with normal staining of Nissl bodies in the control group. **b:** Degeneration with shrinkage and strong staining of Nissl bodies (arrows) in the DLM-treated rats. **c, d** Little or no signs of degeneration of pyramidal neurons (P) with nor-

mal staining of Nissl bodies (arrowheads) in the CMN- and NCMN-treated groups, respectively. Cresyl violet staining, scale bar, 50 μ m (a–d)

The mRNA expression of Nrf2 increased in DLM-treated group by 200% compared to that of the control group. With use of CMN and NCMN, Nrf2 decreased by 24 and 55% compared to that of DLM-treated group. Though, Nrf2 in both groups still higher than that of the control group (126, 33%, respectively).

Relative mRNA level of Bax, Bcl-2 and Bax/Bcl-2 ratio (Table 5)

Compared to the control group, the expression of Bax in DLM-treated group was 144% higher, while the expression of Bcl-2 of this group was 68% lower. With use of CMN, the expression of Bax became 62% higher, while the expression of Bcl-2 became 40% lower as compared to that of the control group. Finally, the expression of Bax in NCMN-treated group was 14% higher, while the expression of Bcl-2 was 15% lower as compared to that of the control group.

Bax/Bcl-2 ratio of DLM-treated group increased 681% as compared to that of the control group. With use of CMN and NCMN, the ratio increased 171 and 37%, respectively, as compared to that of the control group, while the ratio decreased 65 and 82%, respectively, as compared to that of DLM-treated group.

Impairment of learning

The control group showed daily perfections in their abilities to find the hidden platform (escape latency decreased over the training period) and percentage of time spent in the target quadrant increased. The DLM-treated animals showed an impaired acquisition process (escape latency was longer as compared to that of the control group) and percentage of time spent in the target quadrant was shorter as compared to that of the control group. The ability of rats in CMN- and NCMN-treated groups to find the hidden

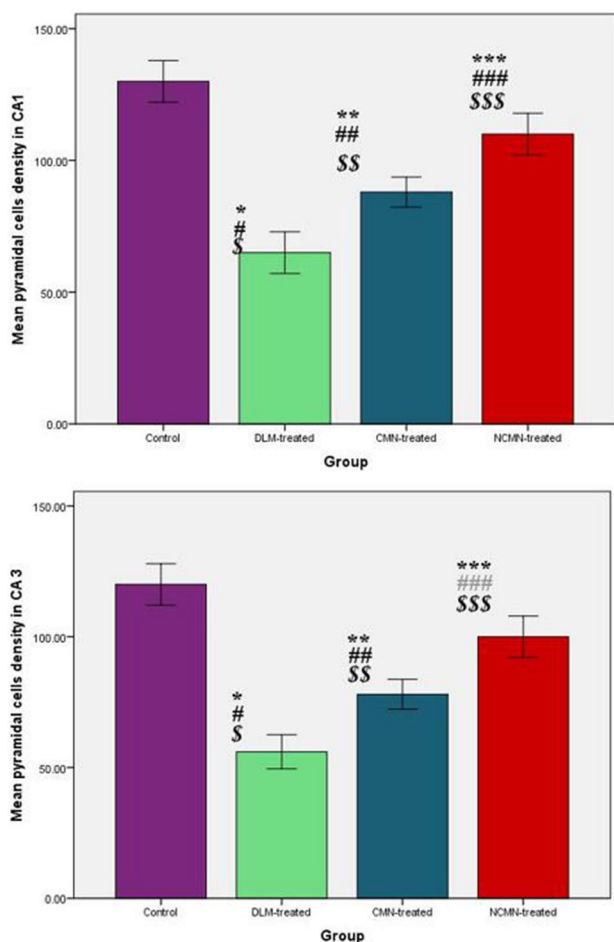


Fig. 5 Bar charts showing pyramidal cell density in CA1 and CA3 areas. The density in DLM-treated group decreased significantly as compared to that of control, CMN- and NCMN-treated groups [$p=0.000$ (*), $p=0.001$ (#), $p=0.000$ (\$), respectively]. Though the density in CMN-treated groups increased as compared to that of DLM-treated group [$p=0.001$ (**)], the density was significantly less than that of the control and NCMN-treated groups [$p=0.000$ (**), (\$\$), respectively]. Finally, the density in NCMN-treated groups was significantly better than that DLM- and CMN-treated groups [$p=0.000$ (***), $p=0.001$ (####), respectively]; however, the density was significantly less than that of the control group [$p=0.000$ (\$\$\$)]

platform displayed much better findings as compared to that of DLM-treated rats. In addition, percentage of time spent in the target quadrant in both groups was longer as compared to that of DLM-treated group. Finally, the behavior performance in NCMN-treated rats was better than that of CMN-treated rats (Fig. 9).

Discussion

In our study, DLM-treated rats looked sick with a significant decrease in their body weight. Such findings could be attributed to direct cytotoxic effect of DLM on somatic cells

leading to malabsorption of nutrients from the gastrointestinal tract (Ball and Chhabra, 1981). Severe deterioration of the general condition with final death was observed in five rats (3/8)(37.5%). The rats' death declined in CMN and NCMN-treated groups to become one rat in each group (1/8) (12.5%). Such decline reflected the overall general protective role of CMN and NCMN against DLM toxicity.

We aimed to prove that oxidative stress is the common mechanism responsible for DLM-induced hippocampal neurotoxicity. As reported by others (Sayeed et al. 2003; Ding et al. 2017), oxidative stress is the one of the mechanisms through which DLM induces its neurotoxicity. It has a negative influence on nervous system (Salim 2017). It is defined as a shift in balance between oxidants and antioxidants in favor of oxidants (Birben et al. 2012). While the use of DLM, MDA (oxidant, lipid peroxidation marker) increased, CAT, SOD and GSH (antioxidant markers) decreased. DLM oxidative damage is the consequence of free radical formation (ROS) (O_2^- , HO^- radicals, and H_2O_2) (Li et al. 2011), with concomitant lipid peroxidation. Generation of ROS may result from reactive metabolites of DLM (Li et al. 2011). The observed increase in SOD is caused by its role in facilitation of spontaneous dismutation of superoxide radicals to generate H_2O_2 , which is further removed by CAT (Saso and Firuzi 2014). GSH is increased as it is a nonenzymatic endogenous antioxidant that offers neutralizing function by chelation of transition metals (Chance et al. 1979).

We measured the transcription factor Nrf2 as it is a chief mediator of oxidative stress response (Li et al. 2011). It is a keystone in cellular defense against oxidants and regulation of oxidative stress detoxification (Mohammadi et al. 2019). Nrf2 increased in DLM-treated group by 200% which is caused by the increase of Nrf2 gene transcription (Li et al. 2011). The toxic insult of DLM with concomitant GSH depletion promoted Nrf2 translocation to nucleus, where it forms a transactivation complex that binds to antioxidant response element (ARE) (Nguyen et al. 2003). Consequently, Nrf2-induced ARE activation directs expression of many genes that combat oxidative stress (Cople et al. 2008).

The cellular level of GSH (γ -glutamyl-cysteinyl-glycine) is determined by the balance of its synthesis rate and its utilization and loss rate (Kaplowitz et al. 1985). γ -Glutamyl cysteine synthetase (GCS) is the major determinant rate of GSH synthesis (Richman and Meister 1975). It is composed of heavy and light subunits. The heavy subunit (HS) exhibits all the catalytic activity of the enzyme, while the light subunit (LS) is enzymatically inactive (Huang et al. 1993). mRNA levels of both subunits were elevated in DLM-treated group. Such elevation was the result of oxidative stress as reported by many researchers (Moinova and Mulcahy 1998, 1999). Consequently, DLM upregulated both HS and LS subunits.

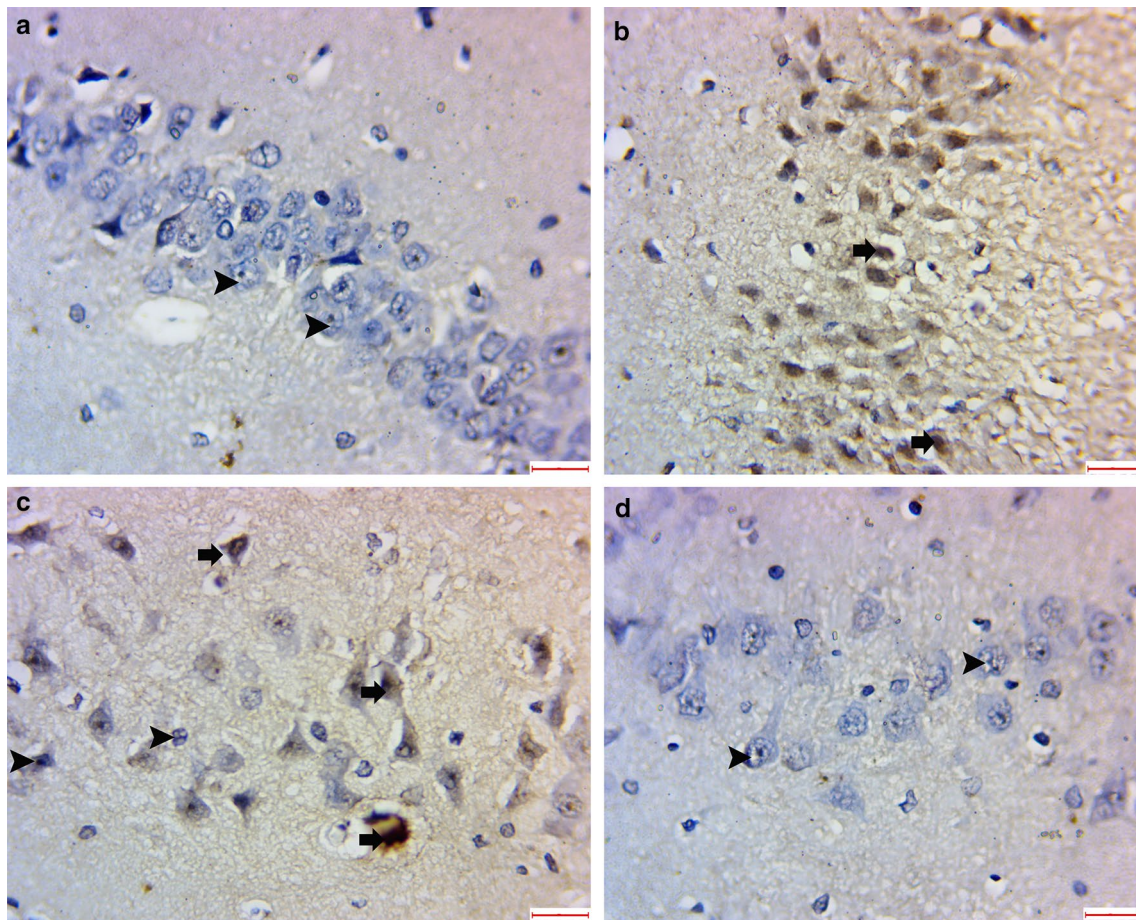


Fig. 6 **a** Absent immunoreaction (arrowheads) in the control group. **b** Dark brown caspase-3-positive cells (arrows) in the DLM-treated rats. **c** Neurons with caspase-3-positive cells (arrows) and -negative

cells (arrowheads) in the CMN-treated rats. **d** Absent immunoreaction (arrowheads) in the NCMN-treated rats. Caspase-3 immunostaining, scale bar, 50 μ m (**a–d**)

AChE is the key enzyme that hydrolyzes acetylcholine and is used as a specific biomarker (Guilhermino et al. 1996). The enzyme level decreased in DLM-treated group by 50% compared to the control group and similar findings were reported by others (de la Torre et al. 2002). AChE is mostly inhibited by ROS which in turn affects neurotransmission in cholinergic synapses (Muthulakshmi et al. 2018).

Structural affection of pyramidal neurons and astrocytes was observed with use of DLM. Nerve cells and astrocytes are susceptible to oxidative stress because of its high oxygen consumption and modest antioxidant defenses (Halliwell 1992). Oxidative stress from exogenous substances could potentially attack DNA and promote genotoxicity, including micronucleus induction, chromosomal and nuclear abnormalities and DNA breaks (Lu et al. 2019). Deltamethrin-exposed rat brain exhibited significantly increased oxidative stress and DNA fragmentation using the diphenylamine and DNA laddering assays (Ogaly et al. 2015). In addition, oxidative stress causes cellular apoptosis (Rai et al. 2015). Deltamethrin induced shrinkage of Nissl bodies with an

eightfold increase in apoptosis nerve cells. Apoptotic effect of DLM over hippocampus was documented in many literatures (Huang et al. 2019; Guo et al. 2008; Li et al. 2004). It is characterized by major changes in nuclear morphology, minor changes in cytoplasmic organelles and overall cell shrinkage with formation of apoptotic bodies. Abnormal neuronal apoptosis has severe effects on the nervous system (Wang et al., 2015). We quantified pyramidal neuron densities in the hippocampal CA1–CA3 regions to prove that the observed induction of apoptosis markers results in a decline in total neuronal cell numbers. DLM induced apoptosis through affecting the caspases system. Caspases, a family of cytoplasmic proteases, play a significant role in the effector phase (no return point) of apoptosis (Rami et al. 2003). 16 different caspases have been recognized (Porter and Jänicke 1999). Caspase-3 is the most abundant of the recognized caspases in the brain (Kuida et al. 1996). It hydrolyzes vital structural and functional proteins of the cell, eventually leading to apoptosis (Li et al. 2015). Many researchers recognized the role of DLM in activation of

Table 2 Comparison of the immunostaining variables among different groups

	Group	Mean \pm SD	Minimum	Maximum	Versus group	P value
Caspase-3 ⁺ cells/six sections/animal	Control	3.0 \pm 1.6	1	5	DLM-treated	0.000*
					CMN-treated	0.011*
					NCMN-treated	1.000
	DLM-treated	27.2 \pm 5.6	20	35	Control	0.000*
					CMN-treated	0.000*
					NCMN-treated	0.000*
	CMN-treated	10.4 \pm 2.19	8	13	Control	0.011*
					DLM-treated	0.000*
					NCMN-treated	0.022*
	NCMN-treated	3.6 \pm 1.1	2	5	Control	1.000
					DLM-treated	0.000*
					CMN-treated	0.022*
GFAP (cells 10 ² /mm ²)	Control	13.6 \pm 1.1	12	15	DLM-treated	0.000*
					CMN-treated	0.000*
					NCMN-treated	0.323
	DLM-treated	37.6 \pm 2.4	35	41	Control	0.000*
					CMN-treated	0.000*
					NCMN-treated	0.000*
	CMN-treated	25.2 \pm 1.9	23	28	Control	0.000*
					DLM-treated	0.000*
					NCMN-treated	0.000*
	NCMN-treated	16 \pm 1.6	14	18	Control	0.323
					DLM-treated	0.000*
					CMN-treated	0.000*

*Significant

caspase-3 in vitro and in vivo (Huang et al. 2019). Caspases mechanism is negatively regulated by Bcl-2 family (Adams and Cory 1998). Bax and Bcl-2 are representative members of this family (Tsujimoto 1998). Bax promotes apoptosis, while Bcl-2 prevents apoptosis (Tsujimoto 1998). Bcl-2/Bax ratio tips the balance toward cell survival or cell death (Oltvai et al. 1993). Compared to the control group, the expression of Bax in DLM-treated group was 144% higher while the expression of Bcl-2 was 68% lower, so DLM upregulates the expression of Bax and downregulates the expression of Bcl-2. Inducing apoptosis of hippocampal neurons by DLM finally leads to impairment of learning and memory (Gasmi et al. 2017; Nieradko-Iwanicka and Borzęcki 2015).

The Nissl staining study suggests imminent changes in rough ER morphology in response to DLM application. The induction of ER stress response was recently described in rat hippocampal neurons after subacute DLM treatment (Hossain et al. 2019). Higher rates of protein folding during ER stress will lead to increased production of ROS. Moreover, one of the consequences of the ER stress response is a misbalance in the expression of pro- and anti-apoptotic protein which was observed in our study.

Astrocytes play a crucial role in homeostasis, including antioxidant protection of neurons (Kimelberg and Nedergaard 2010). One of the pathological signs of neurodegenerative insult is enormous activation of astrocytes that is recognized by an increased expression of GFAP (Zamanian

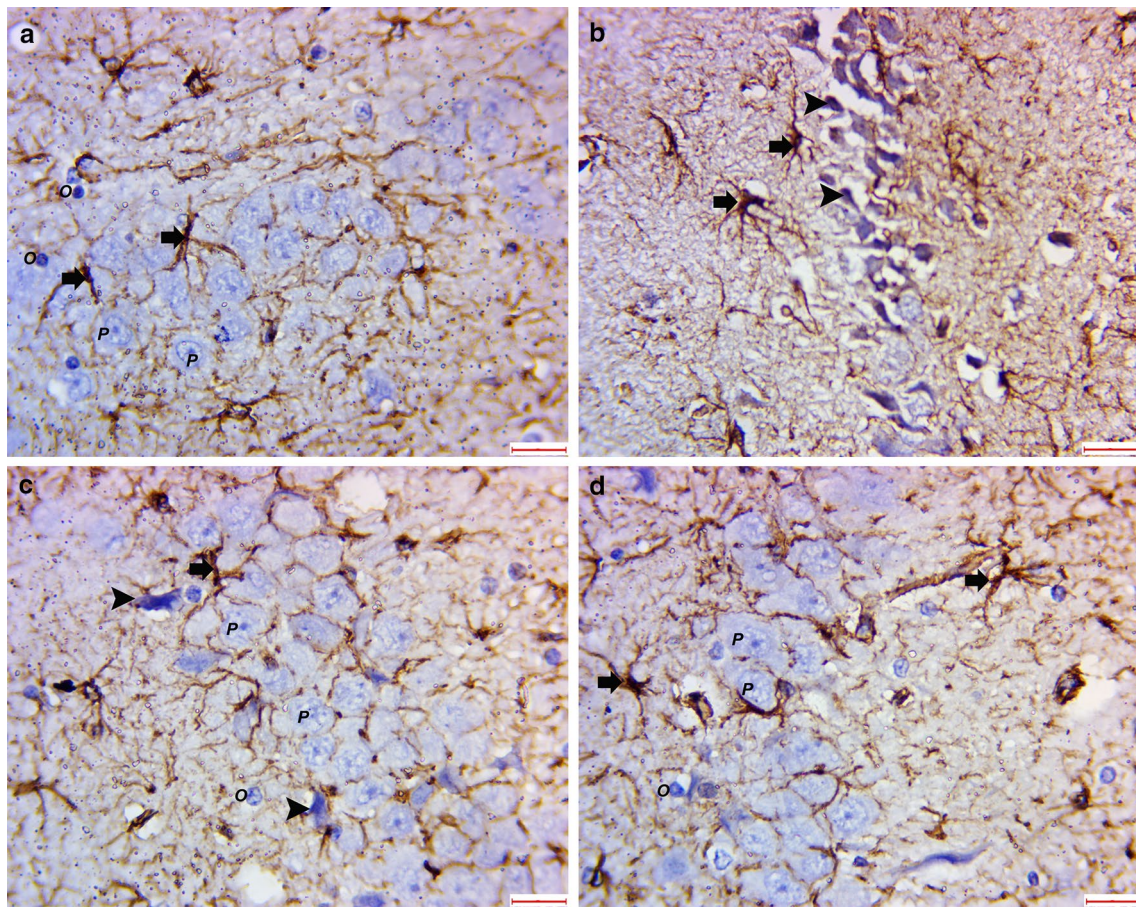


Fig. 7 Dark brown immunoreactive astrocytes (arrows), normal pyramidal neurons (P) and oligodendrocytes (O). **a** Normal immunoreactive astrocytes in the control group. **b, c** Increased number of the immunoreactive astrocytes and apoptotic pyramidal neurons (arrow-

heads) in the DLM- and CMN-treated rats, respectively. **d** Normal immunoreactive astrocytes in the NCMN-treated rats. GFAP immunostaining, scale bar, 50 μm (**a–d**)

et al. 2012). In our work, DLM increased the expression of GFAP by 176%. Many researchers suggested oxidative stress in activation of astrocytes (Daverey and Agrawal 2016). The increased GFAP in DLM-treated group is an early response of astrocytes to protect themselves from oxidative damage.

To determine cognitive dysfunction, hippocampal-dependent learning was evaluated using MWM. DLM-treated animals showed an impaired acquisition process (escape latency was longer as compared to that of the control group) and percentage of time spent in the target quadrant was shorter as compared to that of the control group.

With use of CMN, the number of GFAP and apoptotic neurons decreased as compared to DLM-treated group. The ability of rats in CMN-treated groups to find the hidden platform displayed much better findings as compared to that of DLM-treated rats. In addition, percentage of time spent in the target quadrant was longer as compared to that of DLM-treated group. Finally, behavior performance in NCMN-treated rats was better than that of CMN-treated rats.

The observed protective role of CMN is related to its potent antioxidant effect (Cole, Teter and Frautschy 2007). It exerts its hippocampal protective effect through

Table 3 Comparison of tissue oxidative/antioxidative markers among different groups

	Group	Mean \pm SD	Minimum	Maximum	Versus group	<i>P</i> value
MDA (nmol/mg protein)	Control	6.6 \pm 2.1	4.5	10.0	DLM-treated	0.000*
					CMN-treated	0.000*
					NCMN-treated	0.028*
	DLM-treated	30.0 \pm 4.2	25.2	35.0	Control	0.000*
					CMN-treated	0.000*
					NCMN-treated	0.000*
	CMN-treated	18.4 \pm 1.4	16.7	20.4	Control	0.000*
					DLM-treated	0.000*
					NCMN-treated	0.005*
	NCMN-treated	11.9 \pm 1.0	10.8	13.1	Control	0.028*
					DLM-treated	0.000*
					CMN-treated	0.005*
GSH (U/mg protein)	Control	72.7 \pm 5.3	65.2	78.4	DLM-treated	0.000*
					CMN-treated	0.000*
					NCMN-treated	0.004*
	DLM-treated	27.7 \pm 3.4	24.3	32.7	Control	0.000*
					CMN-treated	0.000*
					NCMN-treated	0.000*
	CMN-treated	47.0 \pm 3.0	43.8	51.2	Control	0.000*
					DLM-treated	0.000*
					NCMN-treated	0.000*
	NCMN-treated	62.5 \pm 3.2	58.2	66.8	Control	0.004*
					DLM-treated	0.000*
					CMN-treated	0.000*
CAT (μ mol/H ₂ O ₂ utilized/min/mg protein)	Control	155.5 \pm 16.0	131.2	173.5	DLM-treated	0.000*
					CMN-treated	0.002*
					NCMN-treated	0.725
	DLM-treated	65.8 \pm 17.0	50.2	93.4	Control	0.000*
					CMN-treated	0.000*
					NCMN-treated	0.000*
	CMN-treated	119.0 \pm 6.8	110.0	127.2	Control	0.002*
					DLM-treated	0.000*
					NCMN-treated	0.052
	NCMN-treated	142.6 \pm 5.5	135.0	149.7	Control	0.725
					DLM-treated	0.000*
					CMN-treated	0.052
SOD (U/mg protein)	Control	17.8 \pm 1.6	16	20	DLM-treated	0.000*
					CMN-treated	0.000*
					NCMN-treated	0.274
	DLM-treated	6.8 \pm 0.8	6	8	Control	0.000*
					CMN-treated	0.001*
					NCMN-treated	0.000*
	CMN-treated	11 \pm 1	10	12	Control	0.000*
					DLM-treated	0.001*
					NCMN-treated	0.000*
	NCMN-treated	16 \pm 1.6	14	18	Control	0.274
					DLM-treated	0.000*
					CMN-treated	0.000*

*Significant

Table 4 Comparison of AChE, GCS-LS, GCS-HS, Nrf2 among different groups

	Group	Mean ± SD	Minimum	Maximum	Versus group	P value
AChE (U/mg protein)	Control	47.0 ± 3.6	41.0	50.0	DLM-treated	0.000*
					CMN-treated	0.001*
					NCMN-treated	0.102
	DLM-treated	23.3 ± 4.8	17.3	29.3	Control	0.000*
					CMN-treated	0.001*
					NCMN-treated	0.000*
	CMN-treated	35.0 ± 2.9	31.0	38.5	Control	0.001*
					DLM-treated	0.001*
					NCMN-treated	0.147
	NCMN-treated	40.8 ± 3.0	36.2	44.2	Control	0.102
					DLM-treated	0.000*
					CMN-treated	0.147
GCS-LS mRNA levels	Control	0.70 ± 0.16	0.5	0.8	DLM-treated	0.000*
					CMN-treated	0.001*
					NCMN-treated	0.250
	DLM-treated	1.68 ± 0.15	1.5	1.9	Control	0.000*
					CMN-treated	0.002*
					NCMN-treated	0.000*
	CMN-treated	1.22 ± 0.19	1.0	1.5	Control	0.001*
					DLM-treated	0.002*
					NCMN-treated	0.071
	NCMN-treated	0.93 ± 0.15	0.7	1.1	Control	0.250
					DLM-treated	0.000*
					CMN-treated	0.071
GCS-HS mRNA levels	Control	0.87 ± 0.08	0.9	1.0	DLM-treated	0.000*
					CMN-treated	0.007*
					NCMN-treated	0.009*
	DLM-treated	1.78 ± 0.31	1.5	2.2	Control	0.000*
					CMN-treated	0.122
					NCMN-treated	0.091
	CMN-treated	1.42 ± 0.26	1.1	1.7	Control	0.007*
					DLM-treated	0.122
					NCMN-treated	1.000
	NCMN-treated	1.4 ± 0.16	1.2	1.6	Control	0.009*
					DLM-treated	0.091
					CMN-treated	1.000
Nrf2 folds	Control	1.5.0 ± 0.3	1.0	1.8	DLM-treated	0.000*
					CMN-treated	0.000*
					NCMN-treated	0.952
	DLM-treated	4.5 ± 0.8	3.5	5.5	Control	0.000*
					CMN-treated	0.039*
					NCMN-treated	0.000*
	CMN-treated	3.4 ± 0.7	2.5	4.0	Control	0.000*
					DLM-treated	0.039*
					NCMN-treated	0.007*
	NCMN-treated	2.0 ± 0.3	1.7	2.5	Control	0.952
					DLM-treated	0.000*
					CMN-treated	0.007*

*Significant

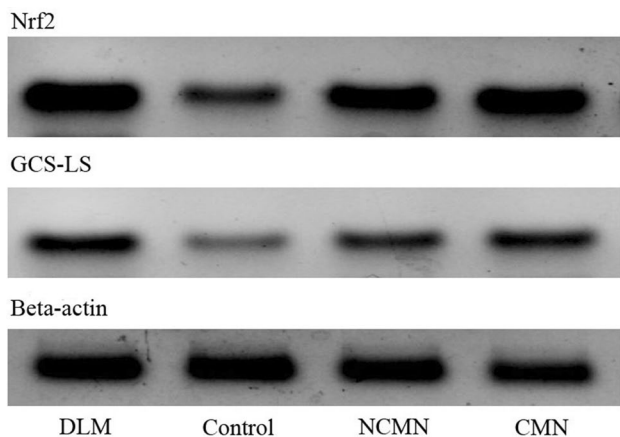


Fig. 8 The mRNA expressions of Nrf2 and GCS-LS in the four groups were analyzed by quantitative real-time RT-PCR. β -actin mRNA was used as internal control to measure the relative quantitation of the expression of the target gene. The expression of both genes increased in DLM-treated group. The expression decreased in CMN-treated groups with more decrease in NCMN-treated group

decreasing oxidants (MDA) and increasing antioxidants (GSH, SOD and CAT). It induces endogenous antioxidant defense mechanism through modulation of Nrf2 (decreased by 24%). In addition, CMN has free radical-scavenging activity (Kocaadam and Şanlıer 2017). CMN inhibits upregulation of DLM over GFAP, HS-GCS and LS-GCS. Much improvement was detected with use of NCMN as it has efficient oral absorption and a better pharmacokinetic profile as compared to CMN (Onoue et al. 2010; Sasaki et al. 2011).

In conclusion, oxidative stress is the common mechanism responsible for DLM-induced hippocampal neurotoxicity. It exerts apoptosis of hippocampal neurons through increasing Nrf2, HS-GCS, LS-GCS and decreasing AChE. In addition, it activates astrocytes through increasing expression of GFAP. Finally, cognitive dysfunction was observed with use of DLM. The protective role of CMN and CMMN is related to their potent antioxidant effect. Better improvement was detected with NCMN as compared to CMN.

Table 5 Comparison of BAX, Bcl-2 and BAX/Bcl-2 ratio among different groups

	Group	Mean \pm SD	Minimum	Maximum	Versus group	P value
Relative mRNA level of Bax	Control	0.77 \pm 0.17	0.55	0.95	DLM-treated	0.000*
					CMN-treated	0.000*
					NCMN-treated	0.863
	DLM-treated	1.88 \pm 0.1	1.75	2.0	Control	0.000*
					CMN-treated	0.000*
					NCMN-treated	0.000*
	CMN-treated	1.25 \pm 0.11	1.1	1.4	Control	0.000*
					DLM-treated	0.000*
					NCMN-treated	0.001
	NCMN-treated	0.88 \pm 0.06	0.8	0.95	Control	0.863
					DLM-treated	0.000*
					CMN-treated	0.001
Relative mRNA level of Bcl-2	Control	1.32 \pm 0.12	1.2	1.5	DLM-treated	0.000*
					CMN-treated	0.000*
					NCMN-treated	0.016*
	DLM-treated	0.42 \pm 0.08	0.3	0.5	Control	0.000*
					CMN-treated	0.000*
					NCMN-treated	0.000*
	CMN-treated	0.78 \pm 0.07	0.7	0.89	Control	0.000*
					DLM-treated	0.000*
					NCMN-treated	0.000*
	NCMN-treated	1.12 \pm 0.08	1.0	1.2	Control	0.016*
					DLM-treated	0.000*
					CMN-treated	0.000*
Bax/Bcl-2 ratio	Control	0.59 \pm 0.15	0.42	0.75	DLM-treated	0.000*
					CMN-treated	0.131
					NCMN-treated	1.000
	DLM-treated	4.61 \pm 1.23	3.5	6.66	Control	0.000*
					CMN-treated	0.000*
					NCMN-treated	0.000*
	CMN-treated	1.6 \pm 0.17	1.37	1.85	Control	0.131
					DLM-treated	0.000*
					NCMN-treated	0.382
	NCMN-treated	0.81 \pm 0.12	0.68	0.95	Control	1.000
					DLM-treated	0.000*
					CMN-treated	0.382

*Significant

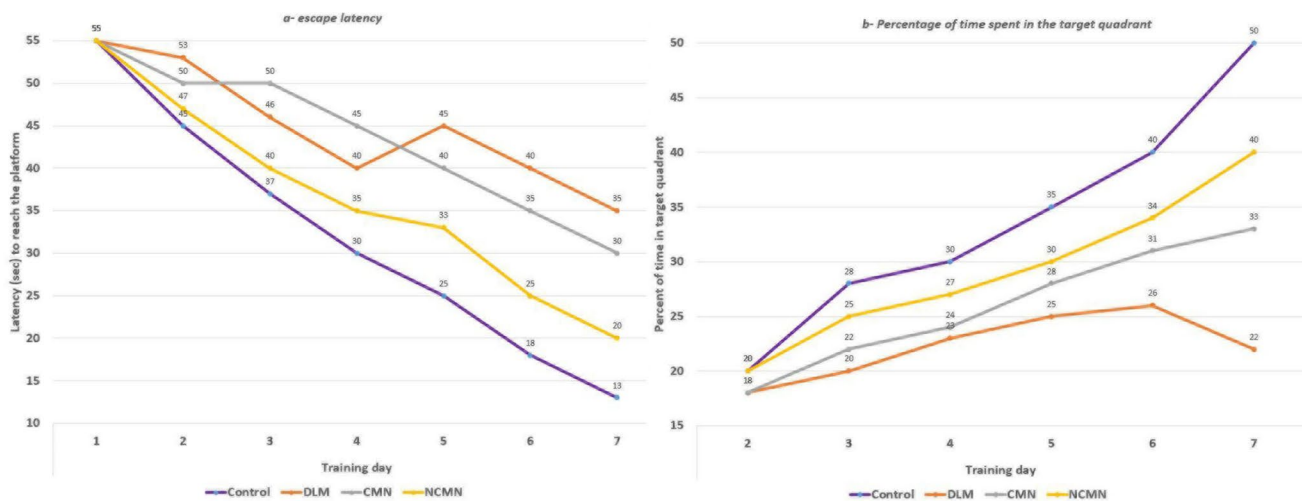


Fig. 9 Spatial learning in the MWM. Spatial learning was assessed as a function of training day with respect to the following parameters: **a** escape latency and **b** percentage of time spent in the target quadrant

Acknowledgements To all my colleagues who supported me during this work.

Compliance with ethical standards

Conflict of interest No conflict of interest.

References

- Adams JM, Cory S (1998) The Bcl-2 protein family: arbiters of cell survival. *Science* 281(5381):1322–1326
- Aebi H (1984) Catalase in vitro. *Methods Enzymol* 105:121–126
- Anand P, Kunnumakkara AB, Newman RA, Aggarwal BB (2007) Bioavailability of curcumin: problems and promises. *Mol Pharm* 4(6):807–818
- Arisi GM (2014) Nervous and immune systems signals and connections: cytokines in hippocampus physiology and pathology. *Epilepsy Behav* 38:43–47
- Ball LM, Chhabra RS (1981) Intestinal absorption of nutrients in rats treated with 2,3,7,8-tetrachlorodibenzo-p-dioxin (TCDD). *J Toxicol Environ Health* 8(4):629–638
- Bhawana, Basniwal RK, Buttar HS, Jain VK, Jain N (2011) Curcumin nanoparticles: preparation, characterization, and antimicrobial study. *J Agric Food Chem* 59(5):2056–2061
- Birben E, Sahiner UM, Sackesen C, Erzurum S, Kalayci O (2012) Oxidative stress and antioxidant defense. *World Allergy Organ J* 5(1):9–19
- Breckenridge CB, Holden L, Sturgess N, Weiner M, Sheets L, Sargent D, Soderlund DM, Choi JS, Symington S, Clark JM, Burr S, Ray D (2009) Evidence for a separate mechanism of toxicity for the Type I and the Type II pyrethroid insecticides. *Neurotoxicology* 30(Suppl 1):S17–S31
- Chance B, Schoener B, Oshino R, Itshak F, Nakase Y (1979) Oxidation-reduction ratio studies of mitochondria in freeze-trapped samples. NADH and flavoprotein fluorescence signals. *J Biol Chem* 254(11):4764–4771
- Cole GM, Teter B, Frautschy SA (2007) Neuroprotective effects of curcumin. *Adv Exp Med Biol* 595:197–212
- Copple IM, Goldring CE, Kitteringham NR, Park BK (2008) The Nrf2-Keap1 defence pathway: role in protection against drug-induced toxicity. *Toxicology* 246(1):24–33
- Daverey A, Agrawal SK (2016) Curcumin alleviates oxidative stress and mitochondrial dysfunction in astrocytes. *Neuroscience* 333:92–103
- de la Torre FR, Ferrari L, Salibián A (2002) Freshwater pollution biomarker: response of brain acetylcholinesterase activity in two fish species. *Comp Biochem Physiol C Toxicol Pharmacol* 131(3):271–280
- Ding R, Cao Z, Wang Y, Gao X, Luo H, Zhang C, Ma S, Ma X, Jin H, Lu C (2017) The implication of p66shc in oxidative stress induced by deltamethrin. *Chem Biol Interact* 278:162–169
- Ellman GL, Courtney KD, Andres V, Feather-Stone RM (1961) A new and rapid colorimetric determination of acetylcholinesterase activity. *Biochem Pharmacol* 7:88–95
- Frank F, Stricker T, Stallmach T, Braegger CP (2000) Helicobacter pylori infection in recurrent abdominal pain. *J Pediatr Gastroenterol Nutr* 31(4):424–427
- Gasmi S, Rouabhi R, Kebieche M, Boussekine S, Salmi A, Toualbia N, Taib C, Bouteraa Z, Chenikher H, Henine S, Djabri B (2017) Effects of Deltamethrin on striatum and hippocampus mitochondrial integrity and the protective role of Quercetin in rats. *Environ Sci Pollut Res Int* 24(19):16440–16457
- Grosse G, Thiele T, Heuckendorf E, Schopp E, Merder S, Pickert G, Ahnert-Hilger G (2002) Deltamethrin differentially affects neuronal subtypes in hippocampal primary culture. *Neuroscience* 112(1):233–241
- Guilhermino L, Celeste Lopes M, Carvalho AP, Soares AM (1996) Inhibition of acetylcholinesterase activity as effect criterion in acute tests with juvenile *Daphnia magna*. *Chemosphere* 32(4):727–738
- Guo L, Sun M, Xu PP, Xu YP, Lu HP, Si HY, Yan H (2008) Effects of melatonin on nerve cell apoptosis and expression of Bcl-2 & cytochrome C genes in rat cerebrum with deltamethrin induction. *Zhonghua Lao Dong Wei Sheng Zhi Ye Bing Za Zhi* 26(4):215–218
- Halliwell B (1992) Reactive oxygen species and the central nervous system. *J Neurochem* 59(5):1609–1623

- Hossain MM, Suzuki T, Sato I, Takewaki T, Suzuki K, Kobayashi H (2005) Neuromechanical effects of pyrethroids, allethrin, cyhalothrin and deltamethrin on the cholinergic processes in rat brain. *Life Sci* 77(7):795–807
- Hossain MM, DiCicco-Bloom E, Richardson JR (2015) Hippocampal ER stress and learning deficits following repeated pyrethroid exposure. *Toxicol Sci* 143(1):220–228
- Hossain MM, Sivaram G, Richardson JR (2019) Regional susceptibility to ER stress and protection by salubrinal following a single exposure to deltamethrin. *Toxicol Sci* 167(1):249–257
- Huang CS, Anderson ME, Meister A (1993) Amino acid sequence and function of the light subunit of rat kidney gamma-glutamylcysteine synthetase. *J Biol Chem* 268(27):20578–20583
- Huang H, Chen X, Li D, He Y, Li Y, Du Z, Zhang K, DiPaola R, Goodin S, Zheng X (2015) Combination of α -tomatine and curcumin inhibits growth and induces apoptosis in human prostate cancer cells. *PLoS ONE* 10(12):e0144293
- Huang X, Liang Y, Qing Y, Chen D, Shi N (2019) Proteasome inhibition by MG-132 protects against deltamethrin-induced apoptosis in rat hippocampus. *Life Sci* 220:76–83
- Kalpana C, Menon VP (2004) Modulatory effects of curcumin on lipid peroxidation and antioxidant status during nicotine-induced toxicity. *Pol J Pharmacol* 56(5):581–586
- Kaplowitz N, Aw TY, Ookhtens M (1985) The regulation of hepatic glutathione. *Annu Rev Pharmacol Toxicol* 25:715–744
- Kimelberg HK, Nedergaard M (2010) Functions of astrocytes and their potential as therapeutic targets. *Neurotherapeutics* 7(4):338–353
- Klaassen CD, Watkins JB, Casarett LJ (2010) *Casarett & Doull's essentials of toxicology*, 2nd edn. McGraw-Hill Medical Pub. Division, New York
- Kocaadam B, Şanlıer N (2017) Curcumin, an active component of turmeric (*Curcuma longa*), and its effects on health. *Crit Rev Food Sci Nutr* 57(13):2889–2895
- Kuida K, Zheng TS, Na S, Kuan C, Yang D, Karasuyama H, Rakic P, Flavell RA (1996) Decreased apoptosis in the brain and premature lethality in CPP32-deficient mice. *Nature* 384(6607):368–372
- Li T, Shi N, Zhong YF, Dong J, Chen L, Wang B, Chen D, Wei YH, Dai ZH (2004) Effects of deltamethrin on the apoptosis and the expression of caspase-3 in rat neural cells. *Zhonghua Lao Dong Wei Sheng Zhi Ye Bing Za Zhi* 22(5):371–374
- Li HY, Wu SY, Ma Q, Shi N (2011) The pesticide deltamethrin increases free radical production and promotes nuclear translocation of the stress response transcription factor Nrf2 in rat brain. *Toxicol Ind Health* 27(7):579–590
- Li H, Wu S, Chen J, Wang B, Shi N (2013) Effect of glutathione depletion on Nrf2/ARE activation by deltamethrin in PC12 Cells. *Arch Hig Rada Toksikol* 64(1):87–97
- Li J, Meng Z, Zhang G, Xing Y, Feng L, Fan S, Fan F, Buren B, Liu Q (2015) *N*-acetylcysteine relieves oxidative stress and protects hippocampus of rat from radiation-induced apoptosis by inhibiting caspase-3. *Biomed Pharmacother* 70:1–6
- Lu WP, Mei XT, Wang Y, Zheng YP, Xue YF, Xu DH (2015) Zn(II)-curcumin protects against oxidative stress, deleterious changes in sperm parameters and histological alterations in a male mouse model of cyclophosphamide-induced reproductive damage. *Environ Toxicol Pharmacol* 39(2):515–524
- Lu Q, Sun Y, Ares I, Anadón A, Martínez M, Martínez-Larrañaga MR, Yuan Z, Wang X, Martínez MA (2019) Deltamethrin toxicity: a review of oxidative stress and metabolism. *Environ Res* 170:260–281
- Mandal MN, Patlolla JM, Zheng L, Agbaga MP, Tran JT, Wicker L, Kasus-Jacobi A, Elliott MH, Rao CV, Anderson RE (2009) Curcumin protects retinal cells from light- and oxidant stress-induced cell death. *Free Radic Biol Med* 46(5):672–679
- Menon VP, Sudheer AR (2007) Antioxidant and anti-inflammatory properties of curcumin. *Adv Exp Med Biol* 595:105–125
- Misra HP, Fridovich I (1972) The role of superoxide anion in the autoxidation of epinephrine and a simple assay for superoxide dismutase. *J Biol Chem* 247(10):3170–3175
- Mohammadi H, Ghassemi-Barghi N, Malakshah O, Ashari S (2019) Pyrethroid exposure and neurotoxicity: a mechanistic approach. *Arch Hig Rada Toksikol* 70(2):74–89
- Moinova HR, Mulcahy RT (1998) An electrophile responsive element (EpRE) regulates beta-naphthoflavone induction of the human gamma-glutamylcysteine synthetase regulatory subunit gene. Constitutive expression is mediated by an adjacent AP-1 site. *J Biol Chem* 273(24):14683–14689
- Moinova HR, Mulcahy RT (1999) Up-regulation of the human gamma-glutamylcysteine synthetase regulatory subunit gene involves binding of Nrf-2 to an electrophile responsive element. *Biochem Biophys Res Commun* 261(3):661–668
- Muthulakshmi S, Maharajan K, Habibi HR, Kadirvelu K, Venkataramana M (2018) Zearalenone induced embryo and neurotoxicity in zebrafish model (*Danio rerio*): role of oxidative stress revealed by a multi biomarker study. *Chemosphere* 198:111–121
- Nguyen T, Sherratt PJ, Pickett CB (2003) Regulatory mechanisms controlling gene expression mediated by the antioxidant response element. *Annu Rev Pharmacol Toxicol* 43:233–260
- Nieradko-Iwanicka B, Borzęcki A (2015) Subacute poisoning of mice with deltamethrin produces memory impairment, reduced locomotor activity, liver damage and changes in blood morphology in the mechanism of oxidative stress. *Pharmacol Rep* 67(3):535–541
- Nunez J (2008) Morris water maze experiment. *J Vis Exp* 19:e897
- Ogaly HA, Khalaf AA, Ibrahim MA, Galal MK, Abd-Elsalam RM (2015) Influence of green tea extract on oxidative damage and apoptosis induced by deltamethrin in rat brain. *Neurotoxicol Teratol* 50:23–31
- Oltvai ZN, Milliman CL, Korsmeyer SJ (1993) Bcl-2 heterodimerizes in vivo with a conserved homolog, Bax, that accelerates programmed cell death. *Cell* 74(4):609–619
- Onoue S, Takahashi H, Kawabata Y, Seto Y, Hatanaka J, Timmermann B, Yamada S (2010) Formulation design and photochemical studies on nanocrystal solid dispersion of curcumin with improved oral bioavailability. *J Pharm Sci* 99(4):1871–1881
- Porter AG, Jänicke RU (1999) Emerging roles of caspase-3 in apoptosis. *Cell Death Differ* 6(2):99–104
- Radovanović TB, Nasia M, Krizmanić II, Prokić MD, Gavrić JP, Despotović SG, Gavrilović BR, Borković-Mitić SS, Pavlović SZ, Saičić ZS (2017) Sublethal effects of the pyrethroid insecticide deltamethrin on oxidative stress parameters in green toad (*Bufo viridis* L.). *Environ Toxicol Chem* 36(10):2814–2822
- Rai P, Parrish M, Tay IJ, Li N, Ackerman S, He F, Kwang J, Chow VT, Engelward BP (2015) *Streptococcus pneumoniae* secretes hydrogen peroxide leading to DNA damage and apoptosis in lung cells. *Proc Natl Acad Sci U S A* 112(26):E3421–E3430
- Rami A, Jansen S, Giesser I, Winckler J (2003) Post-ischemic activation of caspase-3 in the rat hippocampus: evidence of an axonal and dendritic localisation. *Neurochem Int* 43(3):211–223
- Rashid K, Sil PC (2015) Curcumin ameliorates testicular damage in diabetic rats by suppressing cellular stress-mediated mitochondrial and endoplasmic reticulum-dependent apoptotic death. *Biochim Biophys Acta* 1852(1):70–82
- Ray DE (1982) Changes in brain blood flow associated with deltamethrin-induced choreoathetosis in the rat. *Exp Brain Res* 45(1–2):269–276
- Richardson JR, Taylor MM, Shalat SL, Guillot TS, Caudle WM, Hossain MM, Mathews TA, Jones SR, Cory-Slechta DA, Miller GW (2015) Developmental pesticide exposure reproduces features of attention deficit hyperactivity disorder. *FASEB J* 29(5):1960–1972

- Richman PG, Meister A (1975) Regulation of gamma-glutamyl-cysteine synthetase by nonallosteric feedback inhibition by glutathione. *J Biol Chem* 250(4):1422–1426
- Saillenfait AM, Ndiaye D, Sabaté JP (2015) Pyrethroids: exposure and health effects—an update. *Int J Hyg Environ Health* 218(3):281–292
- Salim S (2017) Oxidative stress and the central nervous system. *J Pharmacol Exp Ther* 360(1):201–205
- Sasaki H, Sunagawa Y, Takahashi K, Imaizumi A, Fukuda H, Hashimoto T, Wada H, Katanasaka Y, Kakeya H, Fujita M, Hasegawa K, Morimoto T (2011) Innovative preparation of curcumin for improved oral bioavailability. *Biol Pharm Bull* 34(5):660–665
- Saso L, Firuzi O (2014) Pharmacological applications of antioxidants: lights and shadows. *Curr Drug Targets* 15(13):1177–1199
- Sayeed I, Parvez S, Pandey S, Bin-Hafeez B, Haque R, Raisuddin S (2003) Oxidative stress biomarkers of exposure to deltamethrin in freshwater fish, *Channa punctatus* Bloch. *Ecotoxicol Environ Saf* 56(2):295–301
- Sharma P, Singh R, Jan M (2014) Dose-dependent effect of deltamethrin in testis, liver, and kidney of Wistar rats. *Toxicol Int* 21(2):131–139
- Suvarna SK, Layton C, Bancroft JD (2019) Bancroft's theory and practice of histological techniques, 8th edn. Elsevier, Oxford
- Tipple TE, Rogers LK (2012) Methods for the determination of plasma or tissue glutathione levels. *Methods Mol Biol* 889:315–324
- Tsujimoto Y (1998) Role of Bcl-2 family proteins in apoptosis: apoptosomes or mitochondria? *Genes Cells* 3(11):697–707
- Verschöyle RD, Aldridge WN (1980) Structure-activity relationships of some pyrethroids in rats. *Arch Toxicol* 45(4):325–329
- Wagner-Schuman M, Richardson JR, Auinger P, Braun JM, Lanphear BP, Epstein JN, Yolton K, Froehlich TE (2015) Association of pyrethroid pesticide exposure with attention-deficit/hyperactivity disorder in a nationally representative sample of U. S. children. *Environ Health* 14:44
- Wang Y, Bai C, Guan H, Chen R, Wang X, Wang B, Jin H, Piao F (2015) Subchronic exposure to arsenic induces apoptosis in the hippocampus of the mouse brains through the Bcl-2/Bax pathway. *J Occup Health* 57(3):212–221
- Williams MK, Rundle A, Holmes D, Reyes M, Hoepner LA, Barr DB, Camann DE, Perera FP, Whyatt RM (2008) Changes in pest infestation levels, self-reported pesticide use, and permethrin exposure during pregnancy after the 2000–2001 U.S. Environmental Protection Agency restriction of organophosphates. *Environ Health Perspect* 116(12):1681–1688
- Wolansky MJ, Harrill JA (2008) Neurobehavioral toxicology of pyrethroid insecticides in adult animals: a critical review. *Neurotoxicol Teratol* 30(2):55–78
- Wozniak DF, Olney JW, Kettinger L, Price M, Miller JP (1990) Behavioral effects of MK-801 in the rat. *Psychopharmacology* 101(1):47–56
- Wu A, Ren T, Hu Q, Liu Y (2000) Deltamethrin induces altered expression of P53, Bax and Bcl-2 in rat brain. *Neurosci Lett* 284(1–2):29–32
- Wu A, Li L, Liu Y (2003) Deltamethrin induces apoptotic cell death in cultured cerebral cortical neurons. *Toxicol Appl Pharmacol* 187(1):50–57
- Yan X, Pan B, Lv T, Liu L, Zhu J, Shen W, Huang X, Tian J (2017) Inhibition of histone acetylation by curcumin reduces alcohol-induced fetal cardiac apoptosis. *J Biomed Sci* 24(1):1
- Zamanian JL, Xu L, Foo LC, Nouri N, Zhou L, Giffard RG, Barres BA (2012) Genomic analysis of reactive astrogliosis. *J Neurosci* 32(18):6391–6410
- Zhu Y, Liu F, Zou X, Torbey M (2015) Comparison of unbiased estimation of neuronal number in the rat hippocampus with different staining methods. *J Neurosci Methods* 254:73–79

Publisher's Note Springer Nature remains neutral with regard to jurisdictional claims in published maps and institutional affiliations.